PCCP

Accepted Manuscript

ROYAL SOCIETY OF CHEMISTRY

www.rsc.org/pccp

Journal Name

ARTICLE

A Bifurcated Molecular Pentad Capable of Sequential Electronic Energy Transfer and Intramolecular Charge Transfer

Received 00th January 20xx,
Accepted 00th January 20xx

DOI: 10.1039/x0xx00000x

www.rsc.org/

Anthony Harriman,[a,*] Patrycja Stachelek,[a] Alexandra Sutter[b] and Raymond Ziessel[b,*]

An extended molecular array, comprising three distinct types of chromophore and two additional redox-active subunits, that harvests photons over most of the visible spectral range has been synthesized and characterised. The array exhibits a rich variety of electrochemical waves when examined by cyclic voltammetry but assignment can be made on the basis of control compounds and molecular orbital calculations. Stepwise electronic energy transfer occurs along the molecular axis, corresponding to a gradient of excitation energies, to populate the lowest-energy excited state of the ultimate acceptor. This latter species, which absorbs and emits in the far-red region, enters into light-induced charge transfer with a terminal amine group. The array is relatively stable under illumination with white light but degrades slowly via a series of well-defined steps, the first of which is autocatalytic. One of the main attributes of this system is the capability to harvest an unusually high fraction of sunlight while providing protection against exposure to UV light.

Introduction

In attempting to mimic certain features of natural photosynthesis,[1] especially with respect to the fundamental processes leading to charge separation,[2] an inordinately wide diversity of molecular systems has been examined.[3-8] In the main, these materials are intended to exhibit directed electronic energy transfer (EET) along the molecular axis by way of positioning chromophores according to their respective excitation energies.[9] Other molecular systems[10-15] have been designed to duplicate the efficient light-induced charge transfer (CT) inherent to the natural reaction centre complex. In studying such molecules, much fundamental information has been learned about the factors that control the dynamics of EET and/or CT in artificial systems, although many of the subtleties of the living organism have evaded capture in the form of an artificial analogue. Less attention has been given to the study of molecular architectures that successfully combine EET and CT at the same site, even though certain structures are able to achieve this feat.[16-18] In particular, the vast plethora of molecular dyads, triads, tetrads, etc known to realise a cascade of EET steps contains few examples where the terminal energy acceptor is linked to a redox centre in such a way that charge-transfer chemistry can take place. We now describe a giant molecular pentad as a prototype of this generic field of hybrid EET/CT molecular edifices. Our specific interest in such molecular systems is to engineer photochemical heat engines that might be suitable for solar heating of domestic water supplies.

The target system comprises two pyrene (PYR) residues attached via the boron atom to a conventional boron dipyrromethene (BODIPY) dye. The latter unit is well known[19] to serve as an acceptor for excitation energy localised momentarily on one of the pyrene fragments. An expanded boron dipyrromethene (ExBOD) dye, this differing from BODIPY by way of increased π-conjugation[20] provided by the styryl functions attached at the 3,5-positions, is attached to BODIPY through the respective pseudo-*meso* site. This type of connection, when used in conjunction with methyl groups at the 1,7-positions, ensures that each *meso*-phenylene rings lies essentially orthogonal to the dipyrrin core. The styryl fragments are equipped with a triphenylamine (TPA) residue that is known to be rather easily oxidised[21] in polar solvents. The final piece of the structure consists of a dithiocyclopentane (DTC) unit intended to act as a conduit for CT between TPA and ExBOD. The overall molecule, which adopts a bifurcated geometry because of the nature of the connections, has a fully extended length of 46.7 Å. This molecule is surprisingly soluble in common organic solvents at room temperature and maintains electronic isolation for each of the five critical components, at least according to the computed molecular orbital description to be discussed later.

[a] Molecular Photonics Laboratory, School of Chemistry, Bedson Building, Newcastle University, Newcastle upon Tyne, NE1 7RU, United Kingdom.
[b] Ecole de Chimie, Polymères et Matériaux, 25, rue Becquerel, 67087 Strasbourg, France.

Electronic Supplementary Information (ESI) available: Full experimental details, molecular orbital descriptions for control compounds, kinetic plots and additional spectroscopic output to support the text.

The three main chromophores, namely PYR, BODIPY and ExBOD, combine to harvest light over the wavelength range from 250 to 800 nm while the DTC fragments provide additional protection against UV photons. It will be appreciated that these chromophores have been arranged according to their respective excitation energy levels (PYR>BODIPY>ExBOD) so as to favour a cascade of EET steps following from selective excitation of pyrene.

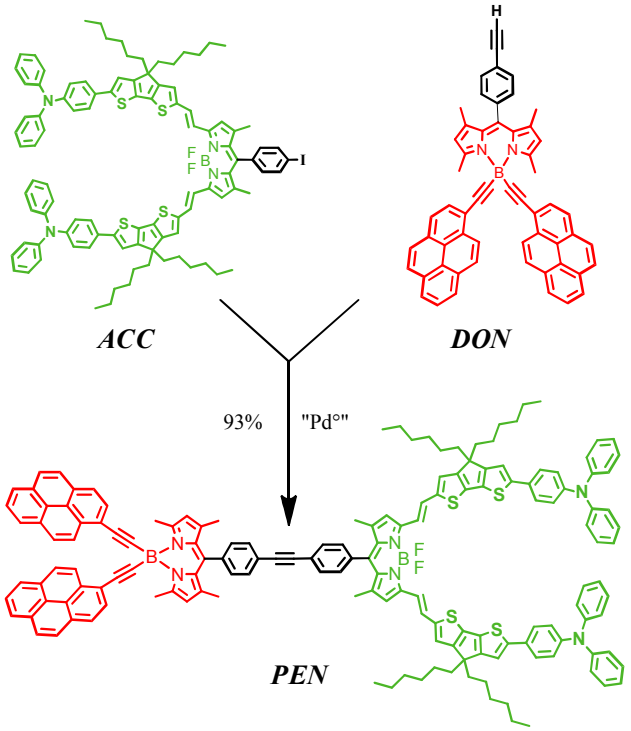

Scheme 1. Synthetic strategy **used** for the preparation of the artificial light harvester PEN **as** examined in this account.

Results and Discussion

Synthesis and Characterisation

The target multi-chromophoric light harvester PEN was prepared according to Scheme 1.[‡] The red (DON) and green (ACC) modules were prepared and purified as described previously[22] and their molecular structures were established unambiguously by NMR spectroscopy. The key cross-coupling reaction between DON and ACC is realized in the presence of catalytic amounts of $[Pd(PPh_3)_4]$ under anaerobic conditions.[23] Purification by column chromatography on flash silica was straightforward and additional purification was ensured by crystallization from appropriate solvents. The highly soluble PEN compound was isolated in 93% yield. The analytically pure compound was analysed by NMR and mass spectroscopies and by elemental composition, unambiguously confirming the molecular structure of the target compound. In particular, the mass analysis revealed a molecular peak at 2281.1 ([M], 100% intensity) with successive fragments assigned to the release of fluorine atoms at 2262.1 ([M-F], 30%) and 2243.1 ([M-2F], 15%). No additional significant fragmentation peaks are observed. A representation of the computed energy-minimised structure is provided as part of the Electronic Supplementary Information.

Cyclic Voltammetry

Cyclic voltammetry studies were conducted with the target compound, PEN, dissolved in deaerated CH_2Cl_2 containing background electrolyte at room temperature. To aid assignment of the various peaks, comparable studies were carried out with the isolated molecular fragments DON and ACC. It was also necessary to consult literature reports for somewhat related BODIPY-based compounds. The main results are summarized by way of Table 1 and indicate the following principal points: Firstly, a single quasi-reversible wave is seen for DON on reductive scans and attributed to formation of the BODIPY-based π-radical anion. The corresponding half-wave potential ($E_{½}$) is -1.42 V vs SCE. For ACC, two waves are seen on reductive scans. The first wave has an $E_{½}$ value of -1.00 V vs SCE but the second wave is electrochemically irreversible and exhibits a cathodic peak potential of -1.63 V vs SCE. It is possible to assign[24] the first reduction wave to formation of the π-radical anion associated with the ExBOD fragment but it is not obvious as to exactly which part of the extended conjugation path is included in the respective molecular orbitals. Likewise, the second wave is not easily attributable to reduction of a particular molecular fragment without further information. The target compound, PEN, exhibits three reductive waves with successive $E_{½}$ values of -1.02, 1.39 and ca. -1.80 V vs SCE. The first two waves are quasi-reversible and can be attributed to one-electron reduction of ExBOD and BODIPY units, respectively. The third wave, this being electrochemically irreversible, occurs at strongly cathodic potentials and appears to be associated with the ExBOD unit. Again, more precise identification demands proper understanding of the nature of the molecular orbitals involved.

Table 1. Summary of the electrochemical properties recorded for ***PEN*** and the two isolated compounds ***ACC*** and ***DON*** in CH_2Cl_2 containing $^{n}Bu_4NPF_6$ as supporting electrolyte.

Compound	$E^{0\prime}$(ox, soln) (V), ΔE (mV)[a)]	$E^{0\prime}$(red, soln) (V), ΔE (mV)[b)]
ACC	+0.38 (60), +0.83 (60), +1.00 (60)	-1.00 (70), -1.63 (irr.)
DON	+0.93 (60), +1.39 (irr.)	-1.42 (60)
PEN	+0.38 (60), +0.83 (60) , +1.29 (irr.)	-1.02 (70), -1.39 (80), -1.80 (irr.)

a) Refers to oxidative processes. b) Refers to reductive processes. c) Irr refers to an irreversible electrochemical step.

On oxidative scans, DON exhibits two waves. The first wave corresponds to formation of the BODIPY-based π-radical cation, this being quasi-reversible, and has an $E_{½}$ value of +0.93 V vs SCE. The second oxidative step is irreversible and appears to be associated with the pyrene unit. In fact, it is well known[25] that one-electron oxidation of aryl hydrocarbons is often followed by rapid association of the π-radical cation with

a neutral molecule, so forming a dimer π-radical cation. Three quasi-reversible waves are observed for ACC under anodic scans. The first wave, having an $E_{½}$ of +0.38 V vs SCE, is most likely associated with the one-electron oxidation of one or both of the TPA units but the remaining two waves cannot be assigned without further information. The same is true for the three oxidative waves associated with PEN. Here, the first wave is quasi-reversible and corresponds to the removal of one electron. The second wave has the appearance of two overlapping peaks and is also quasi-reversible while the third wave is electrochemically irreversible.

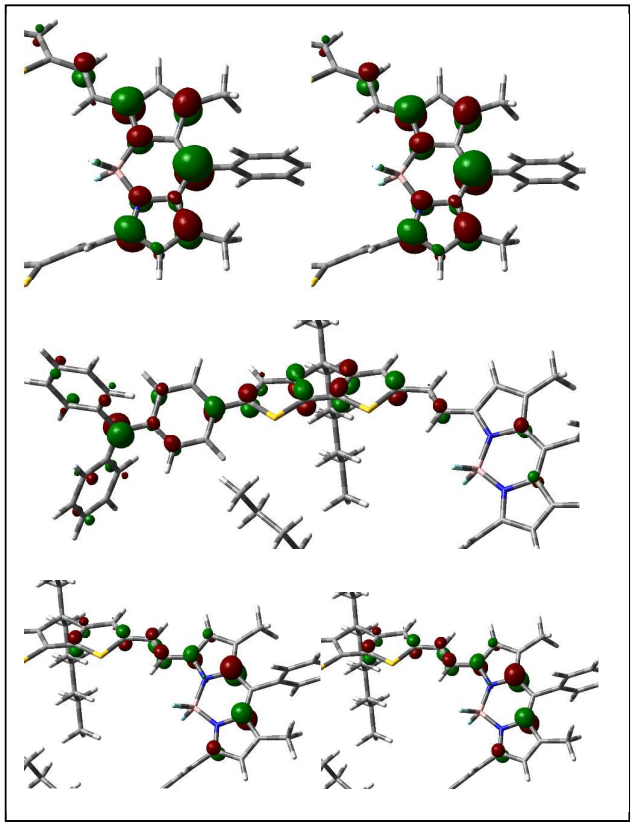

Figure 1. Kohn-Sham representations of LUMO(1) (upper left panel), LUMO (upper right panel), HOMO (centre panel), HOMO(-1) (lower left panel) and HOMO(-3) (lower right panel) for fragments of PEN at an isodensity of 0.02.

In fact, quantum chemical calculations have suggested to us that both LUMO and HOMO associated with DON are localized on the BODIPY unit (Figure S4). Furthermore, HOMO(-1) lies on one of the pyrene units. This situation is entirely in keeping with the above assignment of the cyclic voltammograms. The LUMO associated with ACC is distributed over the styryl-dipyrrin without real penetration onto the DTC units while LUMO(1) appears to be localized on one of the styryl-DTC fragments and is two-fold degenerate (Figure S5). A logical pattern is now apparent for PEN, with the first reduction step being associated with ExBOD and the second with BODIPY (Figure 1). The third reductive step can now be assigned to the irreversible reduction of the tolane-like spacer unit, this being unique to the assembled supermolecule, while the next components in-line for reduction are the two DTC fragments. The LUMO includes an important contribution from the styryl arms and reaches to the first thiophene ring.

The HOMO localized on ACC is essentially centred on one of the TPA fragments (Figure S5), although it stretches onto the attached thiophene ring, and is essentially two-fold degenerate. This finding tends to confirm the above assertion that the observed $E_{½}$ value of +0.38 V vs SCE is due to one-electron oxidation of a terminal TPA unit. According to the MO description, the next component to be oxidized will be ExBOD. Here, the corresponding HOMO reaches onto the styryl arms but not onto the appended DTC units. Thus, one-electron oxidation of ExBOD can be assigned an $E_{½}$ value of +0.83 V vs SCE for ACC. The third wave recognized in the cyclic voltammograms can be attributed to one-electron oxidation of the styryl-DTC fragments and occurs with $E_{½}$ of +1.00 V vs SCE. For the supermolecule PEN, the first oxidation step is clearly associated with the terminal TPA units (Figure 1), as occurs with ACC. The next oxidative process can be safely assigned to one-electron oxidation of the styryl-dipyrrin fragment present in ExBOD. The corresponding $E_{½}$ value becomes +0.83 V vs SCE, exactly as found for ACC. According to the MO descriptors, the two overlapping peaks centred at around 1.3 V vs SCE can be attributed to the successive one-electron oxidation of the DTC fragment and the conventional BODIPY unit, respectively.

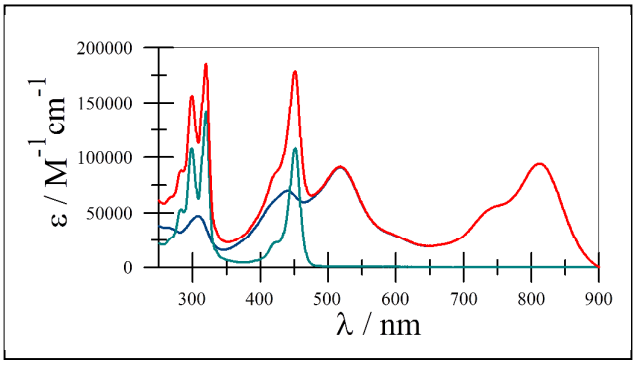

Figure 2. Absorption spectra recorded for PEN (red curve), ACC blue curve) and DON (cyan curve) in CH_2Cl_2 solution.

Absorption and Emission Spectroscopy

The absorption spectrum recorded for PEN in CH_2Cl_2 solution shows a rich variety of optical transitions stretching across the entire visible range and into the near-UV (Figure 2). These transitions can be assigned on the basis of spectra recorded for the reference compounds, with assistance from the scientific literature. Firstly, the absorption transitions associated with ExBOD can be observed at relatively low energy, with the 0,0 band being located at 813 nm and with a pronounced vibronic shoulder at 750 nm. There is essentially no spectral shift between spectra recorded for ACC and PEN over the wavelength region from 550 to 900 nm, thereby indicating that the two BODIPY-based chromophores are not in strong electronic communication. No doubt, the orthogonal phenyl rings help in keeping these chromophores in mutual electronic isolation. The conventional BODIPY dye has a

significant absorption transition centred at 502 nm for DON and at 504 nm for PEN. This transition can be seen clearly in the spectrum recorded for PEN, although there is pronounced spectral overlap with transitions localized on ExBOD. The terminal pyrene chromophores exhibit a series of strong absorption transitions in the near-UV region, giving rise to sharp absorption bands at 276, 286, 351 and 371 nm for PEN (Figure 2). Again, it has to be stressed that these bands are contaminated by weaker absorption due to ExBOD and, to a lesser extent, BODIPY. It is not possible to clearly identify optical transitions associated with either TPA or DTC chromophores, although these are known[26] from earlier studies made with the relevant molecular fragments.

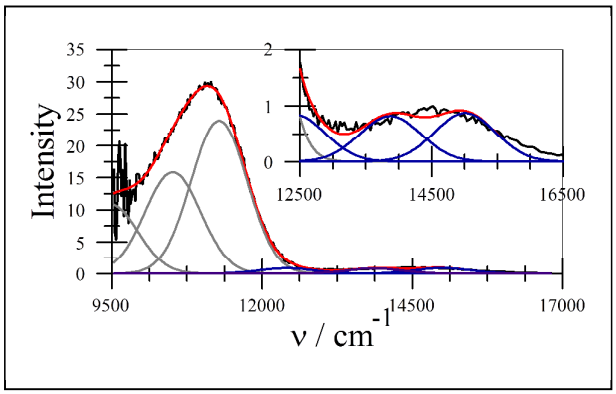

Figure 3. Fluorescence spectrum recorded for PEN in CH_2Cl_2 solution (black curve) and the best fit to a series of Gaussian-shaped vibronic components, with the combined fit shown in red and the individual bands shown in grey. The insert shows the same pattern for the hot emission bands.

Fluorescence can be observed from PEN in CH_2Cl_2 solution following excitation into any of the various chromophores (Figure 3). Thus, excitation at 750 nm gives rise to relatively weak emission centred at about 910 nm that agrees closely with that recorded for ACC under the same conditions. The fluorescence quantum yield (Φ_F), measured in CH_2Cl_2 at room temperature, is 0.013 while the singlet-excited state lifetime (τ_S) measured at 900 nm is 230 ps. The excitation spectrum is in fairly good agreement with the optical absorption spectrum recorded across the entire visible range, although the correspondence is less than perfect in the region around 500 nm. Both Φ_F (= 0.011) and τ_S (= 260 ps) are closely comparable to values recorded for ACC in CH_2Cl_2 solution. In contrast, fluorescence from the BODIPY unit, which is clearly evident at around 515 nm for DON in CH_2Cl_2 solution (Figure S6) where Φ_F = 0.57 and τ_S = 3.7 ns, can hardly be resolved from the baseline. As a crude estimate, emission from the BODIPY fragment present in PEN corresponds to a Φ_F value in the region of 10^{-4} while τ_S (<30 ps) is too short to be resolved by conventional time-correlated, single photon counting methodology. No emission could be attributed to the pyrene fragments,[27] despite the fact that ethynylpyrene emits strongly in the region around 400-440 nm.

An interesting feature of the emission spectra recorded for PEN in CH_2Cl_2 solution at room temperature relates to the pronounced hot fluorescence band seen at ca. 690 nm (Figure 3 insert). For these experiments, the excitation wavelength was 480 nm, corresponding to preferential absorption by the BODIPY unit. The same hot emission is seen for ACC under the same conditions. Spectral curve-fitting analysis, based on the assumption of Gaussian-shaped components, indicates that the spontaneous fluorescence emitted by ExBOD has a major vibronic component of ca. 800 cm^{-1} (Figure 3 insert). The same value is recovered for both PEN and ACC and is independent of excitation wavelength. The hot emission observed for PEN following excitation into the BODIPY unit corresponds to a vibronic mode of ca. 1,460 cm^{-1}. Now, the energy gap between 0,0 vibrational levels for S_1 states associated with the donor and acceptor is 7,540 cm^{-1} but EET is more likely to populate the S_2 state of the acceptor, since the relevant energy gap reduced to 565 cm^{-1}. The remaining excess excitation energy will be lost as rapid intramolecular vibrational cooling and it is here that the 1,460 cm^{-1} mode could play an important role.

Charge Transfer Involving the Terminal ExBOD Unit

Analysis of the cyclic voltammetry results, taken together with the optical absorption and fluorescence data, argues against the occurrence of light-induced charge transfer between the two BODIPY-based chromophores following selective excitation into ExBOD. This situation is confirmed by the observation that both Φ_F and τ_S remain insensitive to the presence of the appended BODIPY unit. Thus, although emission from the ExBOD fragment in both ACC and PEN appears to be heavily quenched, this is not because of interaction with the nearby BODIPY unit. Instead, quenching of the excited-singlet state of ExBOD, in both molecules, is likely to arise from charge transfer from the terminal TPA group (Scheme 2). There is a modest thermodynamic driving force (ΔG = -0.15 eV) for this process in CH_2Cl_2 solution and the interspersed DTC fragment might be expected to function as an effective conduit[28] for intramolecular charge transfer along the molecular axis. This is because the spacer unit is also redox active and could promote through-bond charge transfer by way of super-exchange interactions.[29] It is also important to stress that earlier work[30] has described such light-induced charge transfer in somewhat related molecular architectures.

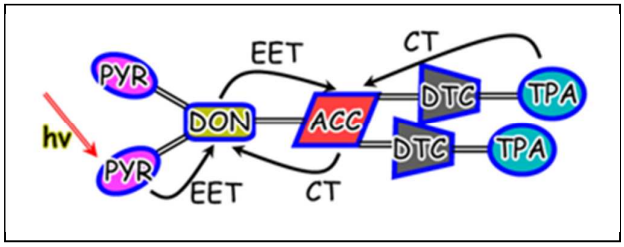

Scheme 2. Simplistic representation of the various events that follow from selective excitation into one of the pyrene units: EET and CT refer, respectively, to electronic energy transfer and light-induced charge transfer.

Pump-probe (FWHM = 120 fs) transient absorption spectroscopy with excitation at 420 nm carried out with ACC in CH_2Cl_2 solution showed the rapid formation of the S_1 state associated with the ExBOD chromophore (Figure 4). This assignment can be made on the basis of the pronounced bleaching at 815 nm and the appearance of stimulated

emission at 900 nm. Decay of the S_1 state follows first-order kinetics, with a lifetime of 225 ± 25 ps, to restore the pre-pulse baseline. There is no obvious indication for transient formation of charge-separated species and, in particular, the TPA radical cation cannot be detected in the spectral window around 740 nm where it is known[31] to display a broad but weak absorption band. The indication, therefore, is that charge recombination (ΔG = -1.30 eV) occurs too quickly for significant build-up of any transient species. In fact, charge recombination is likely to be promoted by super-exchange interactions with the bridging DTC unit. Similar results were observed with PEN in CH_2Cl_2 solution following laser excitation at 420 nm.

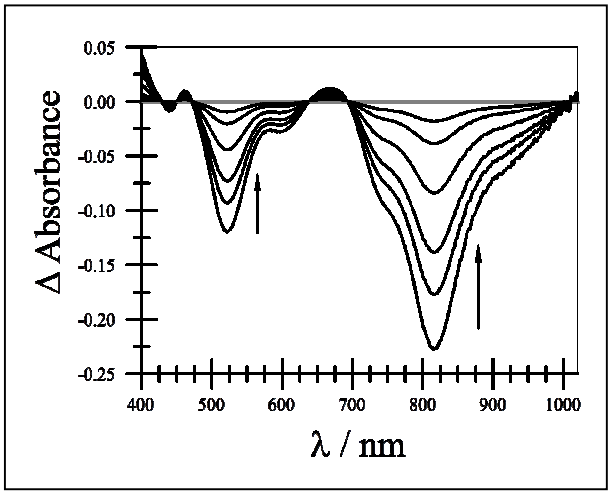

Figure 4. Differential transient absorption spectra recorded following excitation of ACC in deaerated CH_2Cl_2 solution with a short laser pulse at 420 nm: individual traces (average of 100 shots) were recorded at delay times of 0, 55, 110, 215, 350 and 550 ps.

Electronic Energy Transfer along the Molecular Axis

Previous work[19] has established that rapid EET occurs from pyrene to BODIPY in several disparate molecular dyads of comparable structure to DON. Such EET is usually quantitative and this is certainly the case for DON. The excitation spectrum agrees well with the absorption spectrum across the region where the pyrene chromophores absorb strongly and this is highly suggestive of efficacious intramolecular EET. We presume that the absence of fluorescence from the pyrene units present in PEN is also because of highly effective EET across the ethynylene bond. This process has been studied in detail[9,19] in simpler molecular structures, where the timescale for intramolecular EET is on the order of a few ps. There is every indication that the same situation holds for both DON and PEN.

Careful comparison of excitation and absorption spectra recorded for PEN in CH_2Cl_2 leads us to the conclusion that intramolecular EET from BODIPY to ExBOD accounts for about 85% of the fate of the first-excited state. Since fluorescence from S_1 is unimportant for PEN, in contrast to DON where Φ_F = 0.57, it follows that an additional nonradiative process competes with EET. According to the results of the cyclic voltammetry experiments, there is a modest thermodynamic driving force (ΔG = -0.19 eV) for light-induced charge transfer from ExBOD to the first-excited singlet state of BODIPY in CH_2Cl_2 solution. In fact, this is the only allowed charge-transfer process between the two main chromophores. It seems likely that this reaction is responsible for the incomplete match between excitation and absorption spectra. In principle, the occurrence of intramolecular charge transfer can be scrutinised[30] by pump-probe transient absorption spectroscopy but it is essentially impossible to isolate a suitable excitation wavelength in the case of PEN. This is because of the strong spectral overlap between BODIPY and ExBOD in the region around 500 nm, together with the difficulty to generate certain excitation wavelengths. As such, we have not been able to confirm this competition for PEN.

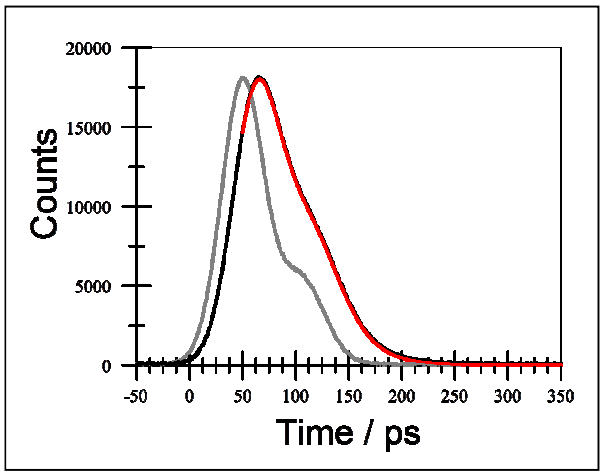

Figure 5. Time-resolved fluorescence decay curve recorded for PEN in CH_2Cl_2 following excitation at 500 nm. The instrumental response function is shown as a grey curve while the fit to the experimental data is shown as a red curve. Emission was detected at 530 ± 25 nm.

The situation is improved when the experiment involves recording time-resolved fluorescence following excitation at 500 nm with a short duration (FWHM = 110 ps) laser diode. Under these conditions, approximately 60% of absorbed photons enter the BODIPY chromophore, with the remaining 40% being partitioned to the ExBOD unit. The latter emits in the far red region but shows no appreciable fluorescence in the wavelength range around 530 nm. Monitoring at this wavelength (Figure 5), which is close to the peak of the emission expected for BODIPY, allows determination of the singlet-excited state lifetime of the latter emitter as being 22 ± 6 ps. The rather large uncertainty arises because of the limited temporal resolution available under these experimental conditions. Taking due account of the comparative excitation spectra, it is now possible to estimate rate constants for intramolecular EET (k_{EET} = 3.9 x 10^{10} s^{-1}) and charge transfer (k_{CT} = 7 x 10^9 s^{-1}) from the first-excited state of BODIPY to ExBOD.

Photochemical Stability

In order to explore the possibilities for developing artificial light-harvesting antennae based on molecular arrays[32] such as

PEN, attention has been given to the inherent photostability of the ExBOD chromophore.[33] Thus, a solution of ACC in deaerated CH_2Cl_2 was exposed to simulated sunlight delivered with a 450 W solar illuminator. At early stages of the reaction, the chromophore bleaches slowly under exposure to white light (Figure 6). A series of isosbestic points is evident during this phase of illumination and similar bleaching rates are found across the entire visible spectral range. Under typical illumination conditions, the initial rate of bleaching is ca. 5 nM min^{-1}. At any given wavelength, the bleaching process gives a poor fit to first-order kinetics but shows much better correlation with an autocatalytic mechanism Figure S7.[34] In this latter case, a product formed during early stages of photolysis enhances the rate of bleaching. Fitting the experimental data to such a mechanism[34] across the entire wavelength range allows calculation of the inherent rate constant (k_0) as being 0.0012 min^{-1} and the rate constant for autocatalysis (k_C) as being 0.0018 μM^{-1} min^{-1}. New products are apparent by way of a broad absorption peak centred at around 720 nm and a sharp absorption band centred at 560 nm. These two absorption bands form at the same rate, which agrees with the rate of bleaching of the ExBOD chromophore and, as such, are considered to be the primary products of the bleaching reaction. On continuing the illumination, both products begin to fade at a relatively fast rate to leave a broad absorption band stretching from about 650 to 350 nm. This secondary bleaching step only proceeds once the bleaching of ExBOD is complete. Both absorption bands bleach via approximately first-order kinetics with the same rate constant (k_B) of 0.0025 min^{-1}.

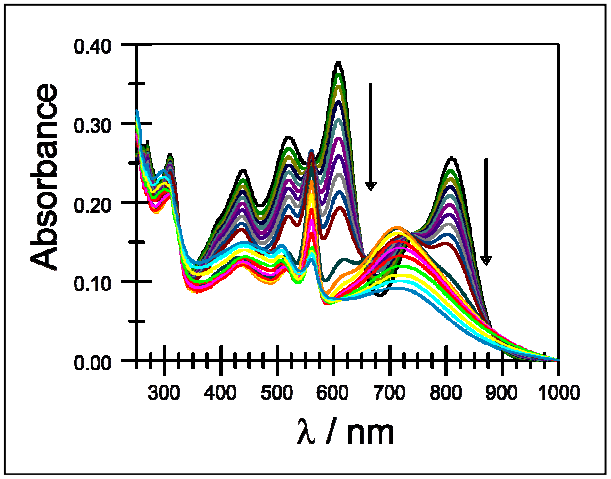

Figure 6. Effect of continuous illumination with white light on the absorption spectrum recorded for ACC in deaerated CH_2Cl_2. The arrows indicate the initial stage of bleaching. Spectra were recorded at regular time intervals over the course of eight hours.

The absorption band seen around 720 nm has the general appearance of a charge-transfer transition while that at 560 nm is what might be expected for an expanded BODIPY derivative possessing limited π-conjugation.[22] Our analysis, however, does not allow identification of the products. An interesting feature of this progressive bleaching chemistry is that both 560-nm and 720-nm absorbing species remain fluorescent so that the ability to sensitise a solar cell or photochemical reaction is entirely not lost and the optical bandgap remains very similar at around 1.4 eV. Furthermore, bleaching of the ultimate product is extremely slow when compared to a solution of Texas Red, the latter being our recommended standard for photochemical bleaching.

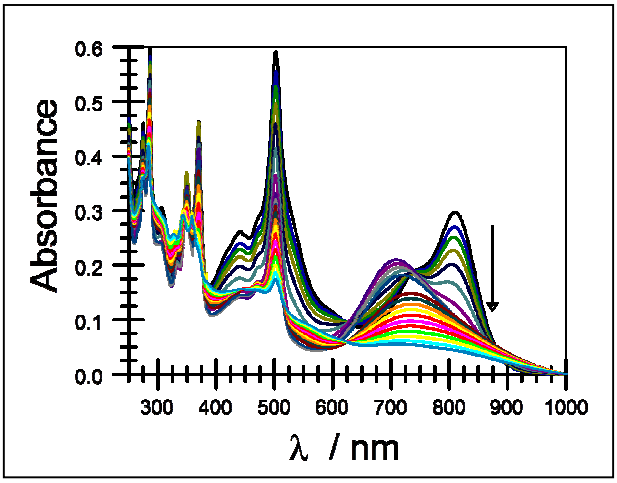

Figure 7. Effect of continuous illumination with white light on the absorption spectrum recorded for PEN in deaerated CH2Cl2. Spectra were recorded at regular intervals over a period of ten hours.

Turning attention to the full array, PEN, in deaerated CH_2Cl_2 solution, it is apparent that illumination with white light causes bleaching of the ExBOD chromophore (Figure 7). As for the control compound, the initial bleaching step corresponds to an autocatalytic reaction (Figure S8).[34] Analysis across the entire spectral window allows derivation of k_0 and k_C, respectively, as being 0.0012 min^{-1} and 0.0049 μM^{-1} min^{-1}. It will be recognised that whereas k_0 remains identical to that found for ACC, the corresponding rate constant for autocatalysis is considerably faster (i.e., almost a factor of 3-fold) for PEN than for ACC despite the fact that bleaching is associated with the ExBOD chromophore in both cases. It can also be seen from the spectral traces that bleaching of ExBOD gives rise to the same charge-transfer absorption band at 710 nm but there is no indication for formation of the absorption band centred at 560 nm. Bleaching of the 710-nm absorption band can be approximated to a first-order process with a rate constant of 0.0032 min^{-1}. Again, this is faster than observed with ACC (k_B = 0.0025 min^{-1}), which might be a consequence of the increased photon flux due to the improved light-harvesting characteristics of PEN compared to ACC. At 502 nm, where both ACC and DON make significant contributions to the total absorbance, the early segment of the bleaching reaction agrees perfectly with autocatalytic bleaching of ExBOD. On longer time scales, the BODIPY chromophores undergoes slow bleaching by approximately first-order kinetics with a rate constant of 0.0019 min^{-1}. It is not practical to monitor bleaching rates for the pyrene chromophore because of the build-up of a permanent product in the near-UV region. This

latter species, which remains fluorescent, bleaches very slowly under white-light illumination.

Attempts were made to follow the bleaching process for PEN using 700-MHz ^{1}H-NMR spectroscopy on a dilute solution (ca. 10^{-4} M). From the data (see Figure S3 for a representative example) some general conclusions can be drawn but the product is a complex mixture of compounds. It appears that the DON part of the PEN chromophore is not damaged at a significant level, according to analysis of the diagnostic signal of the pyrene moiety at 8.63 ppm in CD_2Cl_2. The most fragile part of the molecule, as might be expected, is the ACC fragment which undergoes major modifications of the β-pyrrolic protons. This situation most likely reflects attack of the vinylic system. Several new products are formed as can be testified by the presence of at least three new singlets around 6.0 ppm and new peaks likely assigned, in light of reference compounds, to the dithiocyclopentane fragments. The high intensity of these latter peaks attests the presence of several products displaying similar molecular frameworks.

Conclusions

This work considers the electrochemical, photophysical and photochemical properties of a large supermolecule built up by logical positioning of individual subunits. The assembled array absorbs across the entire visible spectral range and into the near-IR. Essentially, more than 99% of the absorbed photonic energy is converted into heat in less than 1 ns. There are many molecular assemblies that degrade excitation energy into heat but an attractive feature of PEN is that it absorbs over a very wide spectral range. As such, it possesses the main attributes needed for an organic-based photochemical heat engine, provided the material is sufficiently stable under prolonged exposure to sunlight. A key feature of this molecular array is that photodegradation occurs via a series of steps leading to gradual loss of performance. Each of these bleaching steps decreases the fraction of solar light that can be harvested but does not curtail the solar heating process. The net result is that the array functions for extended periods, especially when dispersed in an inert polymer.

The compound displays a rich variety of electrode-active reactions, together with highly efficacious intramolecular EET along the molecular axis. The ExBOD-based acceptor enters into charge-transfer reactions with the terminal amine units, no doubt promoted by super-exchange interactions involving the interspersed dithiocyclopentane unit, such that fluorescence is kept to a modest level. On exposure to sunlight, photons can enter the system at any of the principle chromophores but inevitably reach the ExBOD site and thereby enter into the charge-transfer reaction. The quantum yield for this process is ca. 90%, although the rate is modest, and leads to a transient state possessing around 1.3 eV of redox energy. This charge-transfer state deactivates quickly, at least relative to its rate of formation, thereby serving the purpose of an effective photochemical molecular heating system.

Acknowledgements

We thank Newcastle University and ECPM-Strasbourg for financial support of this work. Further funding from EPSRC (Seed Corn Fund) and CNRS is gratefully acknowledged. We are grateful to Dr. Corrine Wills for recording the NMR traces during photobleaching and to Dr. Anna Gakamsky (Edinburgh Photonics) for recording the far-red emission spectra and lifetimes.

Notes and references

‡ Full experimental details are provided as part of Supporting Information.

1 B. Alberts, A. Johnson, J. Lewis, M. Raff, K. Roberts and P. Walker, Molecular Biology of the Cell, Garland Science, New York, Chap. 14, 2002.

2 J. Fajer, D. C. Brune, M. S. Davis, A. Forman and L. D. Spaulding, *Proc. Natl. Acad. Sci*., 1975, **72**, 4956-4960.

3 J. S. Hsiao, B. P. Krueger, R. W. Wagner, T. E. Johnson, J. K. Delaney, D. C. Mauzerall, G. R. Fleming, J. S. Lindsey, D. F. Bocian and R. J. Donohue, *J. Am. Chem. Soc*., 1996, **118**, 11181-11193. H. E. Song, C. Kirmaier, J. K. Schwartz, E. Hindin, L. H. Yu, D. F. Bocian, J. S. Lindsey and D. Holten, *J. Phys. Chem. B*, 2006, **110**, 19121-19130.

4 J. Iehl, J. F. Nierengarten, A. Harriman, T. Bura and R. Ziessel, *J. Am. Chem. Soc*., 2012, **134**, 831-845. R. Ziessel, G. Ulrich, A. Haefele and A. Harriman, *J. Am. Chem. Soc*., 2013, **135**, 11330-11344.

5 Y. Nakamura, N. Aratani and A. Osuka, *Chem. Soc. Rev*., 2007, **36**, 831-845. J. Yang, M. C. Yoon, H. Yoo, P. Kim and D. Kim, *Chem. Soc. Rev*., 2012, **41**, 4808-4826. I. W. Hwang, N. Aratani, A. Osuka and D. Kim, *Bull. Korean Chem. Soc*., 2005, **26**, 19-31.

6 A. N. Macpherson, P. A. Liddell, D. Kuciauskas, D. Tatman, T. Gillbro, D. Gust, T. A. Moore and A. L. Moore, *J. Phys. Chem. B*, 2002, **106**, 9424-9433. C. Roger, M. G. Muller, M. Lysetska, Y. Miloslavina, A. R. Holzwarth and F. Wurther, *J. Am. Chem. Soc.*, 2006, **128**, 6542-6543.

7 M. J. Leonardi, M. R. Topka and P. H. Dinolto, *Inorg. Chem*., 2012, **51**, 13114-13122. H. Imahori, *J. Phys. Chem. B*, 2004, **108**, 6130-6143.

8 M. S. Choi, T. Yamazaki, I. Yamazaki and T. Aida, *Angew. Chem., Int. Ed*., 2004, **43**, 150-158. F. Wurther, T. E. Kaiser and C. R. Saha-Moeller, *Angew. Chem., Int. Ed*., 2011, **50**, 3376-3410. H. Tamiaki, T. Miyatake, R. Tanikaga, A. R. Holzwarth and K. Schaffner, *Angew. Chem., Int. Ed. Engl*., 1996, **35**, 772-774.

9 R. Ziessel and A. Harriman, *Chem. Commun*., 2011, **47**, 611-631.

10 M. R. Wasielewski, *Acc. Chem. Res*., 2009, **42**, 1910-1921. M. R. Wasielewski, *J. Org. Chem*., 2006, **71**, 5051-5066. V. Balzani, A. Credi and M. Venturi, *ChemSusChem*, 2008, **1**, 26-58. D. Nocera, *Acc. Chem. Res*., 2012, **45**, 767-776. S. Fukuzumi, *Phys. Chem. Chem. Phys*., 2008, **10**, 2283-2297.

11 Y. Nakamura, N. Aratani and A. Osuka, *Chem. Soc. Rev*., 2007, **36**, 831-845. N. Aratani, D. Kim and A. Osuka, *Acc. Chem. Res*., 2009, **42**, 1922-1934. D. M. Guldi, H. Imahori, K. Tamaki, Y. Kashiwagi, H. Yamada, Y. Sakata and S. Fukuzumi, *J. Phys. Chem. A*, 2004, **108**, 541-548.

12 A. Harriman and J.-P. Sauvage, *Chem. Soc. Rev*., 1996, **25**, 41-46. J.-P. Collin, A. Harriman, V. Heitz, F. Odobel and J.-P. Sauvage, *Coord. Chem. Rev*., 1996, **148**, 63-69.

13 D. M. Guldi, *Chem. Soc. Rev*., 2002, **31**, 22-36. F. D'Souza and O. Ito, *Coord. Chem. Rev*., 2005, **249**, 1410-1422. L. Hammarstron, *Curr. Opinion Chem. Biol*., 2003, **7**, 666-673. K.

J. Elliott, A. Harriman, L. Le Pleux, Y. Pellegrin, E. Blart, C. R. Mayer and F. Odobel, *Phys. Chem. Chem. Phys*., 2009, **11**, 8767-8773.

14 M. R. Wasielewski, *Chem. Rev*., 1992, **92**, 435-461. D. Gust, T. A. Moore and A. L. Moore, *Acc. Chem. Res*., 2001, **34**, 40-48. D. Gust, T. A. Moore and A. L. Moore, *Acc. Chem. Res*., 2009, **42**, 1890-1898.

15 L. C. Sun, L. Hammarstrom, B. Akermark and S. Styring, *Chem. Soc. Rev*., 2001, **30**, 36-49. T. S. Balaban, *Acc. Chem. Res*., 2005, **38**, 612-623.

16 A. Harriman and R. Ziessel, *Chem. Commun*., 1996, 1707-1716. M. H. V. Huynh, D. M. Dattelbaum and T. J. Meyer, *Coord. Chem. Rev*., 2005, **249**, 457-483.

17 F. D'Souza, P. M. Smith, M. E. Zandler, A. L. McCarty, M. Itou, Y. Akari and O. Ito, *J. Am. Chem. Soc*., 2004, **126**, 7898-7907. B. Rybtchinski, L. E. Sinks and M. R. Wasielewski, *J. Am. Chem. Soc*., 2004, **126**, 12268-12269.

18 G. Kodis, C. Herrero, R. Palacios, E. Marino-Ochoa, S. Gould, L. de la Garza, R. van Grondelle, D. Gust, T. A. Moore and A. L. Moore, *J. Phys. Chem. B*, 2004, **108**, 414-425. R. Ballardini, A. Credi, M. T. Gandolfi, F. Marchioni, S. Silvi and M. Ventura, *Photochem. Photobiol. Sci*., 2007, **6**, 345-356.

19 A. Harriman, L. J. Mallon and R. Ziessel, *Chem. Eur. J*., 2008, **14**, 11461-11473; A. Harriman, G. Izzet and R. Ziessel, *J. Am. Chem. Soc*., 2006, **128**, 10868-10875; C. Goze, G. Ulrich, L. J. Mallon, D. B. Allen, A. Harriman and R. Ziessel, *J. Am. Chem. Soc*., 2006, **128**, 10231-10239; R. Ziessel, C. Goze, G. Ulrich, M. Cesario, P. Retailleau, A. Harriman and J. P. Rostron, *Chem. Eur. J*., 2005, **11**, 7366-7378.

20 R. Ziessel, P. Retailleau, K. J. Elliott and A. Harriman, *Chem. Eur. J*., 2009, **15**, 10369-10374; M. E. El-Khouly, S. Fukuzumi and F. D'Souza, *ChemPhysChem*, 2014, **15**, 30-47; W.-J. Shi, M. E. El-Khouly, K. Ohkubo, S. Fukuzumi and D. K. P. Ng, *Chem. Eur. J*., 2013, **19**, 11332-11341; F. D'Souza, A. W. Amin, M. E. El-Khouly, N. K. Subbaiyan, M. E. Zandler and S. Fukuzumi, *J. Am. Chem. Soc*., 2012, **134**, 654-664; A. Eggenspiller, A. Takai, M. E. El-Khouly, K. Ohkubo, C. P. Gros, C. Bernhard, C. Goze, F. Denat, J. M. Barbe and S. Fukuzumi, *J. Phys. Chem. A*, 2012, **116**, 3889-3898.

21 C. Lambert and G. Noll, *Synth. Met*., 2007, **139**, 57-62.

22 R. Ziessel, S. Rihn and A. Harriman, *Chem. Eur. J*. 2010, **16**, 11942-11953.

23 A. Sutter and R. Ziessel, *SynLett*. 2014, **25**, 1466-1472.

24 G. Ulrich, R. Ziessel and A. Harriman, *Angew. Chem., Int. Ed. Eng*., 2008, **47**, 1184-1201.

25 J. L. Sessler, Y. Kubo and A. Harriman, *J. Phys. Org. Chem*., 1992, **5**, 644-648.

26 Y. Li, L. Xue, H. Xia, B. Xu, S. Wen and W. Tian, *J. Polym. Sic., Part A. Polym. Chem*., 2008, **46**, 3970-3984.

27 A. Harriman, M. Hissler and R. Ziessel, *Phys. Chem. Chem. Phys*., 1999, **1**, 4203-4211. A. C. Benniston, A. Harriman, D. J. Lawrie and S. A. Rostron, *Eur. J. Org. Chem*., 2004, 2272-2276.

28 K. E. Linton, M. A. Fox, L. O. Palsson and M. R. Bryce, *Chem. Eur. J*., 2015, **21**, 3997-4007.

29 M. N. Paddon-Row, *Aust. J. Chem*., 2003, **56**, 729-748.

30 T. Roland, E. Heyer, L. Liu, A. Rue, S. Ludwigs, R. Ziessel and S. Haacke, *J. Phys. Chem. C*, 2014, **118**, 24290-24301.

31 M. Oyama, N. Nozaki and S. Okazaki, *Anal. Chem*., 1991, **63**, 1387-1392.

32 R. Ziessel, G. Ulrich, A. Haefele and A. Harriman, *J. Am. Chem. Soc*., 2013, **135**, 11330-11344.

33 A. Harriman, P. Stachelek, A. Sutter and R. Ziessel, *Photochem. Photobiol. Sci*., 2015, **14**, 1100-1109.

34 F. Mata-Perez and J. F. Perez-Benito, *J. Chem. Educ*., 1987, **64**, 925-927.

TABLE OF CONTENTS ENTRY

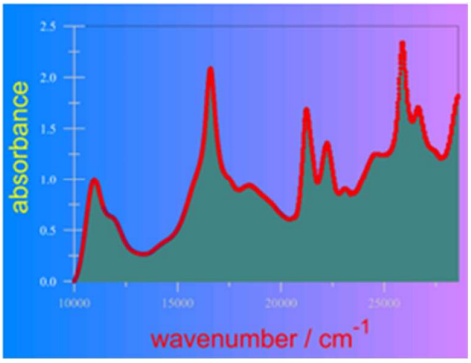

The title compound absorbs strongly over much of the solar range and undergoes a variety of photophysical events under illumination.